Network Lifetime Maximising Distributed Forwarding Strategies in Ad Hoc Wireless Sensor Networks

Bighnaraj Panigrahi†, Swades De†, B. S. Panda‡, and Jean-Daniel Lan Sun Luk*
†Electrical Engineering Department, IIT Delhi, India
‡Mathematics Department, IIT Delhi, India
*Université de la Réunion - Laboratoire LE^{2}P, Saint Denis, Réunion, France

Abstract

We propose three variants of distributed and stateless forwarding strategies for wireless sensor networks, namely, greedy minimum energy consumption forwarding protocol (GMFP), lifetime maximising GMFP (LM-GMFP), and variance minimising GMFP (VAR-GMFP) which aim at maximising the network lifetime while achieving a high forwarding success rate. GMFP selects a forwarding node that minimises per-packet energy consumption while maximising the forwarding progress. LM-GMFP extends the GMFP algorithm by also taking into account the remaining energy at the prospective one-hop forwarding nodes. In VAR-GMFP, on the other hand, the packet is forwarded to the next node that ensures a locally high mean and low variance of nodal remaining energy. Via simple probabilistic analysis we prove the intuition behind the optimum forwarding node selection for network lifetime maximisation. We then model the lifetime maximisation of a sensor network as an optimisation problem and compare the practical protocol-dependent network lifetime with the theoretical upper bound. Through extensive simulations we demonstrate that the proposed protocols outperform the existing energy-aware protocols in terms of network lifetime and end-to-end delay.

Index Terms

Greedy forwarding, location awareness, energy-aware forwarding, network lifetime

I. Introduction

A. Motivation

Wireless sensor networks (WSNs) have gained significant importance in recent years with many application areas, such as transportation, environmental monitoring, health care, national security, and

This work was supported by the Council of Scientific and Industrial Research (CSIR), India, under the grant no. 22/448/07/EMR-II.

structural monitoring. A key challenge in such networks is devising system architectures to realise distributed sensing, data forwarding, and aggregation tasks, subject to hard system constraints, such as limited energy. Due to the difficult environments and a large scale of deployment, recharging or replacing the sensor nodes' batteries may not be feasible. Since there is a high cost associated with the network maintenance caused by frequent battery drainage, energy saving in a WSN to maximise its lifetime has drawn significant attention of the researchers.

As communication range of the field nodes are much smaller compared to the sensing area, field sensor to the sink communication is generally based on multihop forwarding. Also, since the field nodes have limited memory and processing capabilities, distributed control forwarding becomes an obvious choice. Furthermore, if the sensing applications are delay-tolerant, stateless forwarding is practiced, where the nodes do not need to create and maintain routing tables. Typically in the distributed forwarding protocols, local neighbourhood information and the destination location are considered available in some form, e.g., via geographical positioning system (GPS), (e.g., [1]) by other virtual localisation techniques (e.g., [2], [3]). In distributed forwarding, a best relay node is decided at a transmitter from its local neighbours based on various criteria, such as the amount of energy a relay would consume, remaining energy at a candidate node, distance progress toward the destination, link quality between the transmitter and receiver, receiver buffer size, etc.

A common constraint faced by any distributed forwarding strategy in WSN is the wireless channel error. Pure geographic greedy forwarding protocol variants (e.g., [4]–[7]) minimise the source-to-destination hop count by choosing the forwarding nodes at each hop that are as close to the destination as possible. However, this approach may not be optimal in throughput and energy consumption due to more number of retransmissions caused by channel errors. Some other energy-aware routing protocols consider either transmitter energy consumption only [8], [9], or transmitter-receiver energy consumption without accounting the channel errors [10], or energy minimisation without allowing distributed control [11]. In a pure energy-aware forwarding, at every hop the node nearest to the transmitter is selected as the forwarder, as it offers the lowest average number of transmissions per successful packet forwarding. In addition, if the remaining energy of the neighbour node is also considered, then the node with the highest remaining energy will be selected among the nearest nodes [12]. No significant performance gain can be achieved if conversely the minimum energy consuming node is selected from the set of nodes with the highest remaining energy [13]. While the prior protocol level studies have led to prolonging the nodal and network lifetime, we argue that further enhancement of network performance is possible by primarily focusing on the network lifetime maximisation and accounting for the effective energy consumption among the nodes for successful multihop forwarding.

B. Related works

In some energy-efficient forwarding protocols [14]–[17], appropriate cost values are assigned to the forwarding neighbours based on certain criteria. While in [14]–[16] a product of average packet error rate (PER) and distance progress was used as the cost function, the optimisation study in [17] aimed to minimise the average number of retransmissions and at the same time maximise distance progress. However these approaches did not consider the remaining energy of the relay nodes.

The minimum energy path finding approaches proposed in [18], [19] considered link quality as a criteria for route selection. [18] also considered the case with transmit power control. Geographic greediness as well as receiver energy consumption did not play a role in their proposed algorithms. The work in [9] extended the idea of minimum energy routing by accounting the energy consumption due to media access control (MAC) layer control packet exchanges. This approach did not take the receiver energy consumption and link quality in defining the minimum energy routes.

The probabilistic energy-aware routing protocol (which we call PEAR) in [12] defines a cost function considering the energy consumption of transmitter-receiver as well as the remaining energy of the receiver. Here, to decrease the chance of network partitioning, a relay node selection is done randomly based on the assigned probability to a node which is proportional to the energy cost function. A variant of PEAR, called maximum remaining energy directed diffusion (MRE-DD) [13], first selects a set of highest remaining energy nodes and among them chooses the one that would offer minimum energy consumption. Probabilistic geographic routing (PGR) [20] is another such protocol which almost follows PEAR in selecting a relay node in the nearest zone and effectively leads to a higher end-to-end energy consumption. In geographic and energy-aware routing (GEAR) [21], the estimated per-hop forwarding cost is a combination of residual energy and distance to the destination. The network lifetime aware distributed forwarding policy in [22] simultaneously minimises the expected end-to-end delays from all nodes to the sink with the knowledge of the wake-up schedules of the nodes. Without a wake-up scheduling, choosing a forwarding node in this case turns out to be probabilistic and non-optimal. In [23], different network architectures were studied that support max-flow, and two distributed probabilistic on-line routing algorithms were proposed for energy balancing.

In energy aware cluster based protocols (e.g., [24]–[26]) the general idea has been that, at any point in time a fraction of the nodes are elected as the cluster heads for communicating the packets from their neighbouring nodes. In LEACH protocol [24], the network partitioning probability is reduced by randomly rotating the clusterheads. The HEED protocol [25] addressed the nodal residual energy and the scalability limitations of LEACH protocol. In [26], the node with a higher residual energy in the neighbourhood of a clusterhead is assigned a higher probability of being a future clusterhead. A clustering optimisation study was presented in [27], where upper and lower bounds of network lifetime were given with the abstract model of physical layer errors. Some recent clustering protocol studies aimed at network lifetime maximisation [28], [29], where the clusterhead rotation policy as in LEACH [24] was adopted to reduce the remaining energy imbalance in the network. In [28], a neural network based optimum clusterhead election was proposed to dynamically balance the nodal energy consumption and thereby maximising the network lifetime. The approach in [29] obtained optimum number of clusters to cover a sensing area to minimise the energy consumption per cluster as well as the variance of energy consumption among the clusters. While these techniques address the important questions of data aggregation, cluster size, and nodal energy consumption dynamics, they did not consider the physical and MAC layer constraints, such as link quality and packet collisions, and distributed cross-layer performance optimisation aspects.

The authors in [30]–[32] studied distributed cross-layer optimisation and network lifetime maximisation in an interference-limited environment via adaptive link scheduling and optimal rate and power allocation. Along the line of [32], a two-step convex optimisation was formulated in [33] for network lifetime maximisation, which considers transmit power adjustment and varying rate allocation as per the selected receiver's position with respect to the transmitter. A theory was developed for maximising the minimum network lifetime and a centralised algorithm was proposed in [34], where it finds a Pareto optimal solution for the maximum lifetime in an iterative fashion. Alternative frameworks for network lifetime with several different possible lifetime metrics have been discussed in [35], [36].

Our work aims at extending the network lifetime while optimising the distributed forwarding node selection criteria in a network with homogeneous nodal coverage. Unlike the optimisation approaches in [30]–[34], it looks for a joint optimality criteria from the protocol operation viewpoint by combining the factors of greedy geographic forwarding, transceiver energy consumption, nodal residual energy, and link layer retransmission, in data forwarding decision at each hop, which is also different from the protocol-level solutions in [12], [13], [18], [20], [21], [23].

C. Contributions

The current study in this paper considers packet data transmission between any random source-target pairs. We first propose a distributed forwarding criteria, called greedy minimum energy consumption forwarding protocol (GMFP), that minimises transmitter and receiver energy consumption along with maximising Euclidean distance progress towards the destination, where we define a normalised measure called *energy consumption per successful packet forwarding per unit Euclidean distance progress*, E_c. We propose an extension, called lifetime maximising GMFP (LM-GMFP), which, in addition to considering the nodal energy consumption in a successful forwarding, accounts for the remaining energy of the forwarding candidate nodes while choosing an optimum forwarding node. We also propose a heuristic optimisation approach, called variance minimising GMFP (VAR-

GMFP), which tries to maximise the mean energy consumption of the network while minimising the variance of remaining energy of the nodes, thereby attempting to increase the overall lifetime of the network. We formulate a general resource optimisation problem to characterise a multihop forwarding protocol in terms of network lifetime, and compare the longest achievable network lifetime using our proposed forwarding protocols with the theoretical (globally optimal) upper bound. Next, via NS-2 simulations, the network lifetime and throughput performance of the proposed protocols are studied. Our results show that, the proposed protocols outperform the other competitive greedy and energy-aware forwarding strategies in terms of increased nodal and network lifetime without sacrificing the network throughput. The preliminary results of our proposed GMFP and LM-GMFP were presented in [37], [38], where the multihop network lifetime performance and optimisations were not studied.

The possible applications include sending field data from a sensor to a randomly chosen data sink out of several spatially distributed sinks that are deployed for traffic and energy load balancing [39], [40]. This study can be extended to other application-specific sensor networks involving many-to-one communications.

II. Lifetime aware distributed forwarding strategies

In distributed forwarding, the data packets are sent from a source to a target (destination) via multiple hops without having to construct an end-to-end route beforehand. The protocol being stateless, at each hop along a source-destination multihop route the packet forwarding decision is independently taken. The primary objective in our forwarding approach is to maximise the *network lifetime*.

A. System model and notations

We model a static sensor network as a weighted graph $\mathcal{G}(\mathcal{V}, \mathcal{A}, \mathcal{W})$ with $|\mathcal{V}|$ number of sensor nodes, vertex weights $w(x) \in \mathcal{W}, \forall\ x \in \mathcal{V}$, and $|\mathcal{A}|$ undirected links. $(l, m) \in \mathcal{A}$ iff l, $m \in \mathcal{V}$ and both l and m are in the transmission range of each other. $\mathcal{W}$ is the vertex weight set. The sensor nodes are assumed to have homogeneous coverage range and uniformly random distributed in a two-dimensional location space. Each node is aware of its own location information via some localization techniques, e.g., [2], [3], and the one-hop neighbourhood activity status is collected centrally by the relay or in a distributed fashion at the MAC layer (see, e.g., [41]). The sessions are initiated between any source-target pairs. The target location information is known at the source. The effects of imprecise location information on forwarding is not addressed in this work, but a precise location information is not required in the proposed approaches, as a next relay node is selected by the relative measures of the candidate nodes' average distance progress and average reception quality information. In the analysis, network density is assumed sufficiently high so that other than due to energy-depletion routing holes do not arise. Further notations and definitions to characterise the system performance are stated below.

The ith *session* $S^{(i)}\left(s^{(i)}, t^{(i)}, k^{(i)}\right)$ is initiated between a source $s^{(i)}$ and a target $t^{(i)}$, and $k^{(i)}$ is the number of packets to be transmitted in that session. Packets are transmitted only in *slots*, each of duration ξ. *Active transmission* $a_j^{(i)}(l,m)$ is an indicator function that states whether there is an ongoing transmission between two neighbour nodes l and m for the jth packet in session $S^{(i)}$, i.e.,

$$a_j^{(i)}(l,m) = \begin{cases} 1, & \text{if } j\text{th packet transmission in session } i \text{ involves the nodes } l \text{ and } m \\ 0, & \text{otherwise.} \end{cases}$$

Thus, the value of $a_j^{(i)}(l,m) = 1$ only for a selected optimal forwarding neighbour per hop, according to a chosen forwarding protocol. At an intermediate stage of multihop forwarding, i.e., if the target node is not directly reachable from l, a neighbour m is said to be a *potential forwarding neighbour* of l iff $d_{mt^{(i)}} \leq d_{lt^{(i)}}$ and $d_{lm} \leq d_{lt^{(i)}}$, where $t^{(i)}$ is the target node and d_{xy} is the Euclidean distance between node x and y. We denote F_l as the set of all such potential forwarding neighbours of l. *Forward path* $\Phi_j^{(i)}$ is the path followed by the jth packet in the ith session. This path is variable and depends on i and j. *Flow* $f(l,m)$ denotes the number of packets flow between the nodes l and m. The *vertex weight or capacity* $w(l)$ of a vertex l represents the maximum number of packets that can pass through the node l. Throughout the paper, the terms capacity and weight are used interchangeably. *Hop count* $h_j^{(i)}$ is the number of hops taken by the jth packet in the ith session. The tuple (n_1, n_2) denotes a local transmitter-receiver pair, where (n_1, n_2) could take instances as (l,m), or (m,n). $C_j^{(i)}(n_1, n_2, \phi)$ denotes the *cost function* for the jth packet transmission in the ith session at the current node n_1 to one of its neighbours n_2, which is computed differently for different forwarding strategies, depending on whether it is an intermediate stage or a terminal stage of forwarding, as discussed below. ϕ stands for a particular forwarding protocol in use.

B. How to select the next forwarding node?

At each hop, a transmitter has to choose a *next forwarding node* based on certain optimisation criteria. We define a cost function that a distributed forwarding protocol aims to minimise at each hop. A forward direction node having the minimum *cost function* is selected. The forwarding protocols differ by their respective cost functions. Note that, based on the cost function of several potential relaying candidates an optimum node can be *selected* at the transmitter or *elected* via some MAC contention procedure [15]–[17], [42], thereby exploiting the broadcast nature of wireless communication. Below, we characterise how different protocols choose the next forwarding node for the jth packet in the ith session at a node l toward its neighbour m along the forwarding path $\Phi_j^{(i)}$. After each packet transmission/retransmission the transmitter as well as the receiver consume some energy, and so their remaining energy is updated after every attempt.

1) Protocol 1 - GMFP: Greedy Minimum energy consumption Forwarding Protocol: Received power $P_j^{(i)}(l,m)$ at the node m at a distance $d_j^{(i)}(l,m)$ from node l is:

$$P_j^{(i)}(l,m) = \kappa \frac{p_t}{\left[d_j^{(i)}(l,m)\right]^{\gamma}},$$

where p_t is the transmitted signal power, γ is the power law decay factor ($2 \leq \gamma \leq 6$), and κ is a proportionality constant which depends on the transmit and receive antenna properties [43, Ch. 4].

PER $\rho_j^{(i)}(l,m)$ is the probability of a packet being dropped due to link layer errors. PER depends on bit error rate (BER) $\beta_j^{(i)}(l,m)$ which in turn is a function of signal-to-interference-and-noise ratio (SINR) $\Upsilon_j^{(i)}(l,m)$. Assuming a forward error correction coding incorporated at the physical layer that is capable of correcting up to b bit errors in a packet of size L bits, we have:

$$\rho_j^{(i)}(l,m) = 1 - \sum_{e=0}^{b} \binom{L}{e} \left(\beta_j^{(i)}(l,m)\right)^{e} \left(1 - \beta_j^{(i)}(l,m)\right)^{L-e}.$$

With binary phase shift keying (BPSK), for example, $\beta_j^{(i)}(l,m) = \frac{1}{2}\text{erfc}\left(\sqrt{\Upsilon_j^{(i)}(l,m)}\right)$. Interference power $I_j^{(i)}(l,m)$ in a homogeneous nodal transmission coverage scenario can be calculated following the approach in [44], which is a function of the distance $d_j^{(i)}(l,m)$. Approximating the total interference power at a receiver m as Gaussian distributed [45] and denoting the variance of Gaussian channel noise as $\mathcal{N}$, the SINR is obtained as: $\Upsilon_j^{(i)}(l,m) = \frac{P_j^{(i)}(l,m)}{I_j^{(i)}(l,m)+\mathcal{N}}$. For a packet transmission between nodes l and m, one hop throughput $\eta_j^{(i)}(l,m)$ is:

$$\eta_j^{(i)}(l,m) = 1 - \rho_j^{(i)}(l,m).$$

Hence, without retry limit, the expected number of attempts per successful packet from l to m is:

$$R_j^{(i)}(l,m) = \frac{1}{1 - \rho_j^{(i)}(l,m)}.$$

Energy consumption per successful packet forwarding $Es_j^{(i)}(l,m)$ is the total energy spent in successful transmission of a packet from node l to m, which is given by,

$$Es_j^{(i)}(l,m) = (\mathsf{e}_t + \mathsf{e}_r) \cdot R_j^{(i)}(l,m),$$

where e_t and e_r are the respective energy consumed at the transmitter and receiver per transmission attempt. Thus, for successful reception of the jth packet at m, $\mathsf{e}_t \cdot R_j^{(i)}(l,m)$ and $\mathsf{e}_r \cdot R_j^{(i)}(l,m)$ respectively would be the amount of energy consumed by l and m. $Es_j^{(i)}(l,m)$ is the least if m is located in near zone, whereas it is the highest if m is in the far zone (cf. Fig. 1). Finally, the *energy consumption per successful packet per unit Euclidean distance progress* or *normalised energy consumption*, $Ec_j^{(i)}(l,m)$ is,

$$Ec_j^{(i)}(l,m) = \frac{Es_j^{(i)}(l,m)}{d_{p_j}^{(i)}(l,m)},$$

where ${d_p}_j^{(i)}(l,m)$ is the distance progress offered by the node m from the current transmitter l toward the target. Referring to Fig. 1, let $d(A,B)$ is the distance of node B from the current transmitter A, and $\theta(A,B)$ is the angle between A and the baseline joining the transmitter and the destination. Then,

$$d_p(A,B) = d(A,B)\cos\theta(A,B).$$

At the intermediate stage of forwarding, i.e., if the target $t^{(i)}$ is not directly reachable from l, the cost function in the GMFP protocol is defined as:

$$C_j^{(i)}(l,m,1) = Ec_j^{(i)}(l,m).$$

On the other hand, at the terminal stage, i.e., if $t^{(i)}$ is directly reachable from l, we follow a similar strategy as in [19]. The cost function in this case is:

$$C_j^{(i)}(l,m,1) = \begin{cases} Ec_j^{(i)}(l,m) + Ec_j^{(i)}(m,t^{(i)}) & \text{if } m \neq t^{(i)}, \\ Ec_j^{(i)}(l,m) & \text{if } m = t^{(i)}. \end{cases}$$

The optimum next forwarding node, m^* from the transmitter node l is given by,

$$m^* = \underset{m}{\operatorname{argmin}} \;\; C_j^{(i)}(l,m,1).$$

2) Protocol 2 - LM-GMFP: network Lifetime Maximising GMFP: Although GMFP selects a best possible next forwarding node to minimise energy consumption for routing, it does not account for the remaining energy, which may lead to choosing an energy depleted node as a relay, causing an early network partition. LM-GMFP tries to overcome this shortcoming by performing load balancing to increase the individual nodes' as well as overall network's lifetime. Denoting $\tilde{E}^{(r)}(m)$ as the remaining energy of node m, the cost function for LM-GMFP at an intermediate stage of forwarding is defined as:

$$C_j^{(i)}(l,m,2) = \frac{Ec_j^{(i)}(l,m)}{\tilde{E}^{(r)}(m)}.$$

Similarly as in GMFP, at the terminal stage the cost function is modified as:

$$C_j^{(i)}(l,m,2) = \begin{cases} \frac{Ec_j^{(i)}(l,m)}{\tilde{E}^{(r)}(m)} + Ec_j^{(i)}(m,t^{(i)}) & \text{if } m \neq t^{(i)}, \\ Ec_j^{(i)}(l,m) & \text{if } m = t^{(i)}. \end{cases}$$

3) Protocol 3 - VAR-GMFP: Variance minimising GMFP: It minimises the variance of remaining energy of the nodes so as to maximise the lifetime of the network. In this method, we propose a convex function to ensure convergence of the algorithm. Considering only the neighbours of a relay node, let μ_m and ν_m respectively are the mean and variance of remaining energy of the relay node m. We define

$$\Gamma_m = \frac{\zeta \; \mu_m}{1+\nu_m},$$

where ζ is a tunable constant. Here, at the intermediate stage of multihop forwarding, we define the cost function for node l to m transmission as:

$$C_j^{(i)}(l,m,3) = \left(\frac{e_t + e_r}{1 + \eta_j^{(i)}(l,m)\ d_{p_j}^{(i)}(l,m)}\right)^2 + \frac{1}{(1+\mathit{\Gamma}_m)^2}.$$

The next forwarding node selection by this algorithm ensures that the packet should always be forwarded to a region where the mean remaining energy of the nodes is high and variance is low, which would ensure the longevity of the network.

At the terminal stage, since $t^{(i)}$ is already a forward direction neighbour of l, the VAR-GMFP principle does not work; instead the principle of LM-GMFP is followed.

4) Other protocols for comparison: The competitive protocols considered for the performance evaluation of the proposed protocols are greedy geographic least remaining distance (LRD) forwarding [7], GEAR [21], and PEAR [12] protocols.

(a) The cost function in LRD forwarding at the intermediate forwarding stage is:

$$C_j^{(i)}(l,m,LRD) = \frac{1}{d_{p_j}^{(i)}(l,m)}.$$

It is intuitive to note that, at the terminal stage no cost function is computed; instead l attempts to directly deliver the packet to the target.

(b) The cost function in GEAR protocol at the intermediate forwarding stage is:

$$C_j^{(i)}(l,m,GEAR) = \frac{1}{\tilde{E}^{(r)}(m) d_{p_j}^{(i)}(l,m)}.$$

At the terminal stage it is:

$$C_j^{(i)}(l,m,GEAR) = \begin{cases} \frac{1}{\tilde{E}^{(r)}(m) d_{p_j}^{(i)}(l,m)} + \frac{1}{d_{p_j}^{(i)}(m,t^{(i)})} & \text{if } m \neq t^{(i)}, \\ \frac{1}{d_{p_j}^{(i)}(l,m)} & \text{if } m = t^{(i)}. \end{cases}$$

(c) The cost function in PEAR protocol at the intermediate forwarding stage is:

$$C_j^{(i)}(l,m,PEAR) = \frac{Es_j^{(i)}(l,m)}{\tilde{E}^{(r)}(m)}.$$

At the terminal stage of forwarding, it is:

$$C_j^{(i)}(l,m,PEAR) = \begin{cases} \frac{Es_j^{(i)}(l,m)}{\tilde{E}^{(r)}(m)} + Es_j^{(i)}(m,t^{(i)}) & \text{if } m \neq t^{(i)}, \\ Es_j^{(i)}(l,m) & \text{if } m = t^{(i)}. \end{cases}$$

C. *Forwarding node selection zones*

Fig. 2 shows the relation between normalised energy consumption E_c and one hop Euclidean distance progress d_p. It is evident that, for a large transmitter-receiver distance, more energy is consumed due to retransmissions. On the other hand, if the distance to the forwarding node is very small, more energy is consumed due to a higher number of hops from the source to the destination. With these observations we conceptually divide the forwarding area of a node into three different zones: *near*, *middle*, and *far* (cf. Fig. 1). Different distributed forwarding protocols may select a next forwarding node from either of the three zones according to their respective selection criteria.

Computation for a relay node selection is done based on local neighbourhood information (distance between two local neighbours) and long-term average statistics (noise and interference power). In LRD forwarding, the node A will tend to select a node, say the node C, from the *far zone*, whereas by the E_c criteria in GMFP, A will tend to select a node, say the node B or D, from the *middle zone*.

Our proposed two advanced protocols, LM-GMFP and VAR-GMFP, look for the nodes with maximum remaining energy and minimum variance of remaining energy, respectively, from among the minimum E_c nodes. Thus, they will likely select the nodes in the *middle zone*.

III. Network lifetime modelling

Each sensor in the network is provided with a certain initial energy, $\mathcal{E}$. A node is said to be dysfunctional when it does not have enough energy left to transmit, receive, or forward a packet.

Definition 1 (network lifetime): A network is declared to be *dead* when all the forwarding neighbours of a node become energy deficient to forward a packet. We define the life span τ of a network as the total number of successful packets transmitted end-to-end before the network is declared to be dead.

A. Theoretical upper bound on network lifetime

In the network graph $\mathcal{G}$, theoretical upper bound on the maximum number of packet flow between a source-target pair can be obtained by using the max-flow min-cut theorem. We define three lifetime models, namely, *single source, single target* (SSST), *multiple source, single target* (MSST), and *multiple source, multiple target* (MSMT), that encompass all possible data flow cases in a WSN.

The total number of source-set-to-target-set packet flow indicates the network lifetime upper bound. While we discuss the theoretical bounds for all three cases, our system model resembles SSST model. So, SSST is used to compare the theoretical upper bound with the simulated network lifetime.

1) Theoretical lifetime model 1 - SSST: single source, single target: This is the basic model with a single source s and single target node t. Each session has a single packet to transmit between randomly chosen source-target pair. This model is suitable for any-to-any communications.

In order to calculate the theoretical upper bound of network lifetime, we transform the vertex-weighted undirected graph $\mathcal{G}(\mathcal{V}, \mathcal{A}, \mathcal{W})$ into an edge-weighted directed graph $\mathcal{G}'(\mathcal{V}', \mathcal{A}', \mathcal{W}')$ (explained in the Section-III-A4). After constructing $\mathcal{G}'$, the maximum flow capacity of the network is obtained by using the max-flow min-cut theorem.

2) Theoretical lifetime model 2 - MSST: multiple source, single target: In this model, there are a set of source nodes $\mathcal{S}$ and a single target node t. Each session has a single packet to transmit between a randomly selected source node and the fixed target node. As there are a set of source nodes and a single target node, we add an extra virtual source node s^v to the total vertex set and draw edges from s^v to all the nodes in the source set with weights as ∞. Similarly as in SSST, vertex-weighted undirected graph $\mathcal{G}(\mathcal{V}, \mathcal{A}, \mathcal{W})$ is transformed into an edge-weighted directed graph $\mathcal{G}'(\mathcal{V}', \mathcal{A}', \mathcal{W}')$ and then the maximum flow capacity of the network is obtained by using the max-flow min-cut theorem.

3) Theoretical lifetime model 3 - MSMT: multiple source, multiple target: In the MSMT model, in each session only one packet is transmitted between any source-target pair. The procedure of edge-weighted graph construction in this model is similar to that of MSST model with the difference that, instead of a single target node t, there is a set of target nodes $\mathcal{T}$.

4) Construction of weighted directed graph $\mathcal{G}'(\mathcal{V}', \mathcal{A}', \mathcal{W}')$ from $\mathcal{G}(\mathcal{V}, \mathcal{A}, \mathcal{W})$ for MSST model: The $\mathcal{G}'$ construction process in the three models are similar. The process for the generic case of MSST is described below, followed by the max-flow algorithm to find the network lifetime upper bound.

In a sensor network graph, the cost function is generally associated with each node in terms of how many packets can be forwarded through it. We first need to change the vertex-weight set $\mathcal{W}$ into edge-weight set $\mathcal{W}'$. The vertex set $\mathcal{V}$ is split into two identical vertex sets as $\mathcal{V}_1$ and $\mathcal{V}_2$ so that $\mathcal{V}' = \{\mathcal{V}_1 \cup \mathcal{V}_2 \cup \{s^v\}\}$, where $\mathcal{V}_1$ and $\mathcal{V}_2$ are two copies of $\mathcal{V}$, i.e, $\forall\ x \in \mathcal{V}$, we have a copy of x in $\mathcal{V}_1$ as x_1 and another copy in $\mathcal{V}_2$ as x_2. Similarly, each edge in $\mathcal{A}$ is replaced by three new edges in $\mathcal{A}'$, one for each of the two vertices with their capacity equal to the respective vertex capacities, and the third edge between the front side of the first edge to the rear side of the second edge with a capacity of ∞. There could be some redundant edges formed during this construction phase, which can be deleted later. Thus,

$$\mathcal{A}' = \{x_1 x_2 \mid x \in \mathcal{V}\} \cup \{x_2 y_1 \mid y \in F_l(x)\} \cup \{s^v s_1\} \mid s_1 \in \mathcal{S}\},$$

and the corresponding edge-weights are:

$$w'(x_1 x_2) = w(x),\ \forall\ x \in \mathcal{V},$$

$$w'(s^v s_1) = \infty,\ \forall\ s \in \mathcal{S},$$

$$w'(x_2 y_1) = \infty,\ \forall\ y\ \in F_l(x).$$

The construction process is depicted in Fig. 3. As an example, node m in Fig. 3(a) is replaced by an edge (m_1, m_2) with capacity same as that of the node m i.e, c_2. The other nodes along the path from the node s^v to the target node t_2 are also updated as shown in Fig. 3(b). After this transformation, the max-flow min-cut theorem is applied to find the maximum flow between nodes s^v and t_2 which will give the upper bound on network lifetime.

The flow maximisation problem in the transformed max-flow graph $\mathcal{G}'(\mathcal{V}',\mathcal{A}',\mathcal{W}')$ can be stated as:

$$\text{Maximise } |f| = \sum_{\{x:(S^v,x)\ \in\ \mathcal{A}'\}} f(S^v, x)$$

subject to

$$f(l,m) \geq 0 \ \ : \ \ (l,m) \in \mathcal{A}',$$

$$f(l,m) \leq C(l,m) \ \ : \ \ (l,m) \in \mathcal{A}',$$

$$\sum_{\{m:(l,m)\ \in\ \mathcal{A}'\}} f(l,m) - \sum_{\{m:(m,l)\ \in\ \mathcal{A}'\}} f(m,l) = 0 \ \ : \ \ l \in \mathcal{V}' - \{S^v\}, l \neq t_2.$$

The first set of constraints is obvious to account for the nonzero flows only. Second set of constraints states that, at any time the flow value is less than or equal to the edge capacity. The third set of constraints are flow conservation constraints, one for each node. Note that, the modified graph construction and optimisation method for maximising the flows hold for all three theoretical models.

B. Practical lifetime model: Protocol dependent network lifetime

In actual networks it is computationally infeasible to implement the theoretical flow algorithms. Below, we model the network lifetime associated with a practical stateless forwarding algorithm.

The differences in a practical lifetime model are that, it is session-based (instead of flow-based) and protocol-dependent. The first difference tells that, unlike in flows, the sessions are neither partial nor ordered; instead they are complete end-to-end sessions. The second difference signifies that, unlike in the theoretical model, the cost of an edge in practice is not constant; after a transmission or reception of a packet the capacity reduction of a node depends on the protocol in use. In the practical model we have considered both cases: one packet per session and multiple packets per session. In the later case, the ith session is successful if all $k^{(i)}$ packets ($k^{(i)} \geq 1$) are successfully transmitted end-to-end.

Since the energy consumption during the inactive (idling/sleeping) states are much smaller than that in the active states (see, e.g., [46]), we compute the network lifetime by accounting only the time when a node is active in sending, receiving, and forwarding packets, i.e., neglecting the time when there is no sessions running at a node. We define the session-based and protocol-specific network lifetime model as a set of optimisation problems – the feasibility of each one will imply completion of a valid session, at the end of one which, the network lifetime is updated.

In session $S^{(i)}$, average per packet energy consumption by the node l is:

$$\bar{\mathsf{e}}_j^{(i)}(l) = \begin{cases} \sum\limits_{m \in F_l} \mathsf{e}_t \cdot R_j^{(i)}(l,m) \cdot a_j^{(i)}(l,m), & \text{if } l \text{ is a source node,} \\ \sum\limits_{n: l \in F_m} \mathsf{e}_r \cdot R_j^{(i)}(n,l) \cdot a_j^{(i)}(n,l), & \text{if } l \text{ is a destination node,} \\ \sum\limits_{n: l \in F_n} \mathsf{e}_r \cdot R_j^{(i)}(n,l) \cdot a_j^{(i)}(n,l) & \\ \quad + \sum\limits_{m \in F_l} \mathsf{e}_t \cdot R_j^{(i)}(l,m) \cdot a_j^{(i)}(l,m), & \text{if } l \text{ is an intermideate node,} \end{cases}$$

where $R_j^{(i)}(\cdot,\cdot)$ is the average number of retransmissions per successful one-hop progress of a packet, obtained in Section II-B1, and $a_j^{(i)}(\cdot,\cdot)$ is an indicator function, defined in Section II-A to identify an active transmission between two neighbours. If node l actively participates in Π number of sessions in its lifetime, then the total energy consumption by node l is given by

$$\mathsf{e}(l) = \sum_{i=1}^{\Pi} \sum_{j=1}^{k^{(i)}} \bar{\mathsf{e}}_j^{(i)}(l).$$

Definition 2 (valid sessions set, Ψ): A set of sessions is said to be *valid* with respect to the network's initial energy state if, after the completion of the sessions, all nodes in it have non-negative remaining energy. With $k^{(i)}$ packets transmitted in session i, the total number transmitted is $\mathsf{n}(\Psi) = \sum_{i=1}^{|\Psi|} k^{(i)}$.

At each hop, the next node is selected following a chosen forwarding protocol criteria, and its corresponding energy consumption determines the remaining energy of a node for the next packet transmission. The network lifetime τ is the maximum value of i up to which the above optimisation is feasible. Considering the ith session, the valid session set satisfies the following constraints:

$$\begin{aligned}
&\text{a packet to be transmitted successfully} \\
\text{subject to} \quad & \\
& k^{(i)} > 0 : \; 1 \le i \le |\Psi|, \\
& \bar{\mathsf{e}}_j^{(i)}(l) \le \mathcal{E} - \left(\sum_{i'=1}^{i-1} \sum_{j'=1}^{k^{(i')}} e_{j'}^{(i')} - \sum_{j'=1}^{j-1} e_{j'}^{(i')} \right), \quad \forall\, j, \forall\, l \in \Phi_j^{(i)}, \\
& \mathcal{E} - \left(\sum_{i'=1}^{i-1} \sum_{j'=1}^{k^{(i')}} e_{j'}^{(i')} - \sum_{j'=1}^{j-1} e_{j'}^{(i')} \right) \ge 0, \quad \forall\, l \in \Phi_j^{(i)}.
\end{aligned}$$

The first set of constraint is because every session has nonzero, positive number of packets to transmit. The second set of constraints ensures the availability of sufficient residual energy for transmission, in which the left hand side specifies the energy required for transmission of packet j in session i, and the right hand side calculates the remaining energy until the current session. In this case, the network lifetime is the sum of all packets successfully transmitted for the maximum value of number of valid sessions i up to which the above optimisation is feasible. Thus, by Definition 2, $\tau = \mathsf{n}(\Psi)$.

IV. Simulation results and discussion

The network performance evaluation has been carried out via discrete event simulations using network simulator, NS-2.31. We have developed NS-2 patches for our protocols by modifying the existing NS-2 patch for GPSR by [47]. The sensor nodes are deployed in a 300×300 m^2 area uniformly randomly with a network density $\delta = 0.016$ per m^2. We have taken relatively high node densities to avoid routing holes. If routing holes are still encountered, our implementation of the proposed protocols as well as the reference protocols follow perimeter route as in GPSR [4], [47].

Since our primary focus in this work has been providing a proof of concept of our proposed network lifetime maximising forwarding protocols, we did not emphasise on a more advanced detour protocols as in [48], [49], which can be considered for performance efficiency in case of sparse networks where the nodes would encounter routing holes more frequently. To have a BER $\leq 10^{-3}$, transmit power p_t for different transmission radii (20 m to 50 m) were calculated by using two ray ground propagation model with a fixed receiver threshold of -80 dBm, carrier sense threshold of -86 dBm, and long-term average noise power as -86.7 dBm. Sensor node specifications were taken from the Chipcon RFIC CC2420 data-sheet [46]. Log-normal channel fading was simulated with a 4 dB standard deviation. BPSK modulation with NRZ signal was considered. Fixed packet size of $L = 320$ bits was taken and the number of recoverable bit errors was taken $b = 16$ bits, with the transmission time of the packet being $\xi = 4.21$ ms. These values correspond to the existing standard coding mechanism. The initial energy of each node was taken as $\mathcal{E} = 50$ J. To avoid boarder effects, only the nodes within inner $(300 - R) \times (300 - R)$ m^2 region were considered for selecting the source and destination nodes. Sufficient simulation runs were conducted with varying seed values to have a confidence level of 95% within the range of $\pm 2\%$ of the results obtained.

We have considered three performance criteria for comparing the different forwarding protocols: (i) end-to-end throughput η, (ii) nodal energy consumption due to packet transmission and reception, and (iii) network lifetime τ. In our simulations, the consumption during idling/sleep states were ignored as there are negligible compared to that due to packet transmission and reception. Also, since our goal has been to study the relative performance measure of the proposed protocols, the consumption at the network initialisation stage was ignored. Results were taken by generating traffic between randomly chosen source-destination pairs. Each session was considered to transmit a random number of packets between 1 to 5. The network is said to be partitioned at the instant when a transmitter find that none of its forwarding neighbours have sufficient energy to forward a packet. Network lifetime for different forwarding strategies were measured by counting the completed sessions in the simulation time until the network was partitioned.

A. *Effect of nodal coverage range, for a fixed network density*

The three set of plots in Fig. 4 capture relative performance of the competitive protocols at different nodal communication range, R. Fig. 4(a) demonstrates the benefit of LM-GMFP forwarding in terms of reduced energy consumption along the active routes, where it shows that the LRD, PEAR, and GEAR protocols have significantly higher energy consumption. This has an impact on the network lifetime, which is shown in Fig. 6. The increasing trend in energy consumption is because of a much higher transmission power to increase R. Although a higher transmission power helps reduce number of hops to the destination (as noted in Fig. 4(c)), thereby increasing end-to-end success probability

(Fig. 4(b)), the overall consumption due to the increased transmit power leads to an increased energy consumption per packet delivery. It can also be observed from the Fig. 4(c) that PEAR tends to select a forwarding node from the *near zone*, LRD and GEAR choose from the *far zone*, whereas GMFP, LM-GMFP, and VAR-GMFP select from the *middle zone*. As a result, the effect of increased R is most prominent on LRD and GEAR protocols, whereas it is the least in the PEAR protocol.

B. Effect of network density, for a fixed nodal coverage range

To see the impact of change in node density on the performance of these protocols, we have also studied by varying the average number of neighbours with a fixed communication radius, as shown in Fig. 5. Although the results show a little variation at a relatively low network density, the effect of node density on network performance (energy consumption per successful end-to-end per packet delivery in Fig. 5(a) and throughput performance in Fig. 5(b)) is fairly small. This is because, beyond a certain increased node density, the best candidate as per the chosen protocol is nearly achieved. Here also, the lower energy consumption in the GMFP protocol variants is apparent. The hop count in PEAR (Fig. 5(c)) shows an opposite trend because, the tendency to choose nodes from the near zone is aided by the increase in node density, leading to a higher number of hops.

C. Network lifetime and delay performance

Fig. 6 shows that, LRD and GEAR clearly do not help increase the network lifetime. PEAR protocol has a slightly better performance because of its remaining energy awareness. But, due to its tendency of nearby node selection (to reduce loss rate), it consumes more energy in end-to-end delivery via more number of intermediate nodes. The GMFP, LM-GMFP, and VAR-GMFP protocols offer better performances than the other competitive strategies. While achieving reduced variance of remaining energy of nodes, the VAR-GMFP wastes some energy, possibly by detouring from a more energy optimal path offered by LM-GMFP.

However, as observed in Table I, although LM-GMFP gives maximum lifetime compared to GMFP and VAR-GMFP, VAR-GMFP maximises mean and reduces the variance of remaining energy, which is very important while network reconfiguration. LRD protocol has the worst performance figures which is obviously because of its energy unawareness.

The average one hop distance progress at different node densities is compared in Fig. 7. It can be observed from the Fig. 7 that, in PEAR protocol the average distance progress reduces with increase in node density, because it tries to select the next forwarding node from the *near zone*. The other protocols offer an increased one-hop progress with node density. The rate of increase in LRD and GEAR are the highest because they choose the next forwarding node from the *far zone*. These observations further corroborate the trends in Fig. 5(c).

TABLE I

NUMERICAL COMPARISON OF MEAN, VARIANCE, AND NETWORK LIFETIME OF DIFFERENT PROTOCOLS. $R = 40$ M, INITIAL ENERGY PER NODE $\mathcal{E} = 50$ J.

Average number of neighbours →	20	40	60	20	40	60	20	40	60
Forwarding protocol ↓	mean (J)			variance (J^2)			lifetime		
LRD	48.1	47.1	46.73	43.7	46.2	50.9	51	58	112
GEAR	42.2	41.1	39.1	45.1	48.2	49.2	98	116	162
GMFP	42.3	40	39	52.3	41.4	50.5	866	1619	2795
LM-GMFP	37.5	33.2	31.3	98.8	117.5	131	1563	4233	6463
VAR-GMFP	45	43.9	41.5	31.1	26.6	17.2	1422	3764	5821
PEAR	39.5	37.7	35.4	128.9	124.7	117.5	475	1134	2010

The average end-to-end delay of different strategies are shown in Fig. 8. It is observed that although LRD and GEAR take the least number of hops to the destination, they still take a longer time in end-to-end delivery of packets successfully because of a higher number of retransmissions. This observations are also apparent from the Figs. 4(b) and 5(b).

D. Comparison of practical network lifetime with the theoretical upper bound

Because of computational constraints, we have considered SSST model here for the theoretical upper bound calculation, whereas for the practical model, with the same topology, the best protocol in terms of network lifetime, LM-GMFP, has been considered. Also, the theoretical as well as the simulation set-up was implemented on GCC platform. To make the comparison fairer, in the simulations we have not considered retransmissions. In an area of 60×60 m^2 area, we have generated results by taking connected graphs (networks) of varying sizes.

Fig. 9 contrasts the theoretical upper bound on network lifetime with that obtained via practical simulation. Two distinct traits are observed here. First, there is some difference between the theoretical results and the simulated ones. Second, as the network (graph) size increases, in contrast with the theoretical value, there is less change in actual result. These respective differences can be attributed to two reasons. In simulation, a network is declared dead if a node locally finds all its forwarding neighbours do not have the minimum required energy for forwarding, whereas the theoretical results are obtained from a *global* energy-aware max-flow algorithm to find out the maximum possible number of packet flow between a source-destination pair, even if there may exist some nodes who have all their forwarding neighbours energy-depleted. Also, as the size of the graph increases, there is a significant increase in number of additional edges that aids increase of max-flow and hence network lifetime, when it is computed without regard to any fixed protocol. In practice, on the other hand, a protocol-dependent approach has a lesser impact of the additional edges because of its preference to select a forwarding node out of a smaller set of nodes satisfying a chosen forwarding criteria.

V. Concluding Remarks

In this paper we have investigated energy-aware, distributed, and stateless forwarding strategies in wireless multihop sensor networks, where the forwarding node selection criteria is locally optimised based on minimum energy consumption greedy forwarding and nodal remaining energy. We have proposed three variant protocols, namely, GMFP, LM-GMFP, and VAR-GMFP. While GMFP selects a forwarding node on the basis of minimum energy per successful packet transmission per unit Euclidean distance progress toward the destination, LM-GMFP also considers the highest possible remaining energy among the selected node. VAR-GMFP, on the other hand, tries to minimise the overall variance and maximise the mean of remaining energy of the nodes. We have formulated the network lifetime maximisation as a constraint optimisation problem, and compared the protocol-dependent optimum solution with the theoretical upper bound. The performance of the proposed protocols have been compared with the other competitive greedy geographic and energy-aware forwarding techniques. Our extensive simulation based performance results show that the proposed protocols perform significantly better in terms of network lifetime as well as end-to-end delay.

In our future work, we plan to analyse the proposed protocol performances in relatively sparse networks, which can be applicable to distributed control wireless local area networks. We also intend to study the network lifetime characteristics of the forwarding protocols and the resultant optimum deployment patterns in other application-specific sensor networks, such as many-to-one applications, without as well as with distributed transmit power control.

References

[1] N. Bulusu, J. Heidemann, and D. Estrin, "GPS-less low cost outdoor localization for very small devices," *IEEE Personal Commun. Mag.*, vol. 7, no. 5, pp. 28–34, Oct. 2000.

[2] A. Caruso, S. Chessa, S. De, and A. Urpi, "GPS free coordinate assignment and routing in wireless sensor networks," in *Proc. IEEE INFOCOM*, Miami, FL, USA, Mar. 2005.

[3] G. S. Kuruoglu, M. Erol, and S. Oktug, "Localization in wireless sensor networks with range measurement errors," in *Proc. Adv. Intl. Conf. Telecommun.*, Venice, Italy, May 2009.

[4] B. Karp and H. T. Kung, "GPSR: Greedy perimeter stateless rounting for wireless networks," in *Proc. ACM MobiCom*, Aug. 2000, pp. 243–254.

[5] P. Bose, P. Morin, I. Stojmenovic, and J. Urrutia, "Routing with guaranteed delivery in ad hoc wireless networks," *ACM/Springer Wireless Networks*, vol. 7, no. 6, pp. 609–616, Nov. 2001.

[6] M. Zorzi and R. Rao, "Geographic random forwarding (GeRaF) for ad hoc and sensor networks: Multihop performance," *IEEE Trans. Mobile Computing*, vol. 2, no. 4, pp. 337–348, Oct.-Dec. 2003.

[7] S. De, "On hop count and Euclidean distance in greedy forwarding in wireless ad hoc networks," *IEEE Commun. Letters*, vol. 9, no. 11, pp. 1000–1002, Nov. 2005.

[8] S. Singh, M. Woo, and C. Raghavendra, “Power aware routing in mobile ad hoc networks,” in *Proc. ACM/IEEE Mobicom*, Dallas, Texas, USA, Oct. 1998, pp. 181–190.

[9] J. Zhu, C. Qiao, and X. Wang, “A comprehensive minimum energy routing protocol for wireless ad hoc networks,” in *Proc. IEEE INFOCOM*, Hong Kong, China, Mar. 2004.

[10] V. Rodoplu and T. Meng, “Minimum energy mobile wireless networks,” *IEEE J. Sel. Areas in Commun.*, vol. 17, no. 8, pp. 1333–1344, Aug. 1999.

[11] S. Doshi, S. Bhandare, and T. X. Brown, “An on-demand minimum energy routing protocol for a wireless ad hoc network,” *ACM Mobile Comp. and Commun. Rev.*, vol. 6, no. 3, July 2002.

[12] R. C. Shah and J. M. Rabaey, “Energy aware routing for low energy ad hoc sensor networks,” in *Proc. IEEE WCNC*, Mar. 2002, pp. 350–355.

[13] A. K. Hwang, J. Y. Lee, and B. C. Kim, “Design of maximum remaining energy constrained directed diffusion routing for wireless sensor networks,” in *Proc. Intl. Conf. Computational Science and Its Applications, (ICCSA)*, vol. 1, May 2006, pp. 788–795.

[14] J. Kuruvila, A. Nayak, and I. Stojmenovic, “Hop count optimal position based packet routing algorithms for ad hoc wireless networks with a realistic physical layer,” in *Proc. IEEE Intl. Conf. Mobile Ad Hoc and Sensor Systems*, Fort Lauderdale, FL, USA, Oct. 2004.

[15] K. Seada, M. Zuniga, A. Helmy, and B. Krishnamachari, “Energy-efficient forwarding strategies for geographic routing in lossy wireless sensor networks,” in *Proc. ACM SENSYS*, Baltimore, MD, USA, Nov. 2004, pp. 108–121.

[16] M. Souryal and N. Moayeri, “Channel-adaptive relaying in mobile ad hoc networks with fading,” in *Proc. IEEE SECON*, Santa Clara, CA, USA, Sept. 2005.

[17] K. Egoh and S. De, “A multi-criteria receiver-side relay election approach in wireless ad hoc networks,” in *Proc. IEEE MILCOM*, Washington, DC, USA, Sept. 2006.

[18] I. Stojmenovic and X. Lin, “Power-aware localized routing in wireless networks,” *IEEE Trans. Parallel and Distributed Systems*, vol. 12, no. 11, pp. 1122–1133, Nov. 2001.

[19] S. Banerjee and A. Misra, “Minimum energy paths for reliable communication in multi-hop wireless networks,” in *Proc. ACM MOBIHOC*, Lausanne, Switzerland, June 2002, pp. 146–156.

[20] T. Roosta, “Probabilistic geographic routing protocol for ad hoc and sensor networks,” in *Proc. Intl. Wksp. Wireless Ad Hoc Net.*, May 2005.

[21] Y. Yu, R. Govindan, and D. Estrin, “Geographical and energy aware routing: a recursive data dissemination protocol for wireless sensor networks,” UCLA, Tech. Rep., May 2001.

[22] J. Kim, X. Lin, N. B. Shroff, , and P. Sinha, “Minimizing delay and maximizing lifetime for wireless sensor networks with anycast,” *IEEE/ACM Trans. Networking*, vol. 18, no. 2, pp. 515–528, Apr. 2010.

[23] A. Jarry, P. Leone, O. Powell, and J. Rolim, “Optimal data gathering paths and energy balance mechanisms in wireless networks,” *Elsevier Ad Hoc Networks*, vol. 9, no. 6, pp. 1036–1048, Aug. 2011.

[24] W. R. Heinzelman, A. Chandrakasan, and H. Balakrishnan, “Energy-efficient communication protocol for wireless microsensor networks,” in *Proc. Hawaii Intl. Conf. System Sciences*, Maui, HI, USA, Jan. 2000, pp. 366–379.

[25] O. Younis and S. Fahmy, “Heed: A hybrid, energy-efficient, distributed clustering approach for ad hoc sensor networks,” *IEEE Trans. Mob. Comput.*, vol. 3, no. 4, pp. 366–379, Oct.-Dec. 2004.

[26] M. Liu, J. Cao, G. Chen, and X. Wang, “An energy-aware routing protocol in wireless sensor networks,” *Sensors*, vol. 9, no. 1, pp. 445–462, Jan 2009.

[27] V. Shah-Mansouri and V. W. S. Wong, “Bounds for lifetime maximization with multiple sinks in wireless sensor networks,” in *Proc. IEEE Conf. Commun., Comput., and Sig. Proc.*, Victoria, BC, Canada, Aug. 2007.

[28] M. Cordina and C. J. Debono, “Maximizing the lifetime of wireless sensor networks through intelligent clustering and data reduction techniques,” in *Proc. IEEE WCNC*, Budapest, Hungary, Apr. 2009.

[29] H. Li, J. Cao, and J. Xiong, “Constructing optimal clustering architecture for maximizing lifetime in large scale wireless sensor networks,” in *Proc. IEEE Intl. Conf. Parallel and Distributed Sys.*, Shenzhen, China, Dec. 2009.

[30] S. Cui, R. Madan, A. Goldsmith, , and S. Lall, “Joint routing, MAC, and link layer optimization in sensor networks with energy constraints,” in *Proc. IEEE ICC*, Seoul, South Korea, May 2005, pp. 725–729.

[31] R. Madan, S. Cui, S. Lall, and A. Goldsmith, “Cross-layer design for lifetime maximization in interference-limited wireless sensor networks,” *IEEE Trans. Wireless Commun.*, vol. 5, no. 11, pp. 3142–3152, Aug. 2006.

[32] R. Madan and S. Lall, “Distributed algorithms for maximum lifetime routing in wireless sensor networks,” *IEEE Trans. Wireless Commun.*, vol. 5, no. 8, pp. 2185–2193, Aug. 2006.

[33] V. Shah-Mansouri and V. W. S. Wong, “Distributed maximum lifetime routing in wireless sensor networks based on regularization,” in *Proc. IEEE GLOBECOM*, Washington, DC, USA, Nov. 2007, pp. 598–603.

[34] J. C. Dagher, M. W. Marcellin, and M. A. Neifeld, “A theory for maximizing the lifetime of sensor networks,” *IEEE Trans. Commun.*, vol. 55, no. 2, pp. 323–332, Feb. 2007.

[35] A. Giridhar and P. Kumar, “Maximizing the functional lifetime of sensor networks,” in *Proc. ACM Symp. Information Processing in Sensor Networks (IPSN)*, Los Angeles, CA, USA, Apr. 2005, pp. 5–12.

[36] I. Dietrich and F. Dressler, “On the lifetime of wireless sensor networks,” *ACM Trans. Sensor Networks*, vol. 5, no. 1, pp. 1–39, Feb. 2009.

[37] B. Panigrahi, S. De, and J.-D. Lan Sun Luk, “A greedy minimum energy consumption forwarding protocol for wireless sensor networks,” in *Proc. IEEE COMSNETS-IAMCOM*, Bangalore, India, Jan. 2009.

[38] B. Panigrahi, S. De, B. Panda, and J.-D. Lan Sun Luk, “Energy-efficient greedy forwarding protocol for wireless sensor networks,” in *Proc. Vehicular Tech. Conf. (VTC-Spring)*, Taipei, Taiwan, May 2010.

[39] H. Kim, Y. Seok, N. Choi, Y. Choi, , and T. Kwon, “Optimal multi-sink positioning and energy-efficient routing in wireless sensor networks,” *Lecture Notes in Computer Science (LNCS)*, vol. 3391, pp. 264–274, 2005.

[40] Y. Bi, N. Li, and L. Sun, “DAR: An energy-balanced data-gathering scheme for wireless sensor networks,” *Elsevier Computer Communications*, vol. 30, no. 14-15, pp. 2812–2825, Oct. 2007.

[41] K. Egoh and S. De, “Priority-based receiver-side relay election in wireless ad hoc sensor networks,” in *Proc. IEEE Wireless Commun. and Mobile Comp. Conf.*, Vancouver, Canada, July 2006.

[42] M. Zorzi and R. Rao, “Geographic random forwarding (GeRaF) for ad hoc and sensor networks: Energy and latency performance,” *IEEE Trans. Mobile Computing*, vol. 2, no. 4, pp. 349–365, Oct.-Dec. 2003.

[43] T. Rappaport, *Wireless Communications: Principles and Practice*. Prentice Hall, Upper Saddle River, NJ, 2nd ed., 2002.

[44] A. Sharma, B. Panigrahi, and S. De, “Impact of interference on nodal communication range in wireless ad hoc networks,” in *Proc. Nat. Conf. Commun. (NCC)*, Bangalore, India, Jan. 2011.

[45] S. Verdu, *Multiuser Detection*. Cambridge University Press, Cambridge, UK, 1998.

[46] *CC2420 data sheet*, 2006. [Online]. Available: http://www.chipcon.com/files/CC2420_Data_Sheet_1_4.pdf

[47] K. Liu. [Online]. Available: http://www.cs.binghamton.edu/ kliu/research/ns2code/index.html

[48] Q. Fang, J. Gao, and L. J. Guibas, “Locating and bypassing holes in sensor networks,” *Mob. Network Applications*, vol. 11, pp. 187–200, 2006.

[49] F. Yu, S. Park, Y. Tian, M. Jin, and S. Kim, “Efficient hole detour scheme for geographic routing in wireless sensor networks,” in *Proc. IEEE VTC Spring*, Singapore, May 2008.

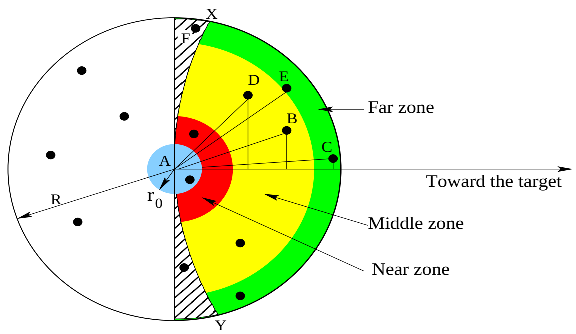

Fig. 1. Forwarding approach dependent node selection zones. r_0 is the near field distance within which range a forwarding node cannot be selected. R is the nodal transmission range.

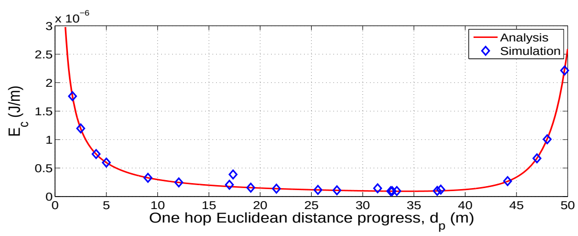

Fig. 2. Energy consumption E_c per successful packet per unit Euclidean distance progress versus Euclidean distance progress d_p. Nodal communication range $R = 50$ m, average number of neighbours $= 50$.

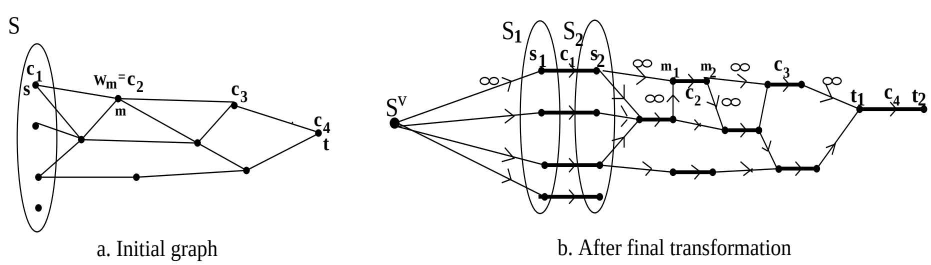

Fig. 3. Construction of edge-weighted, directed graph $\mathcal{G}'$ from a vertex-weighted, undirected graph $\mathcal{G}$.

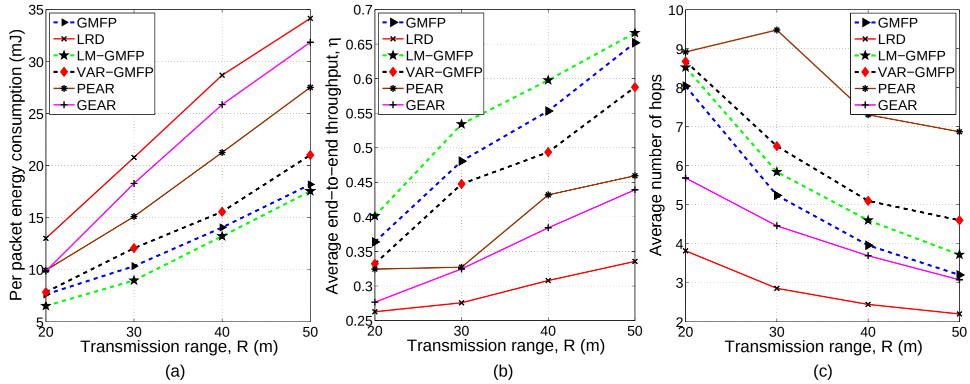

Fig. 4. Nodal transmission range dependent network performance: (a) energy consumption per successful end-to-end packet delivery; (b) end-to-end throughput (probability of success); (c) average hop count.

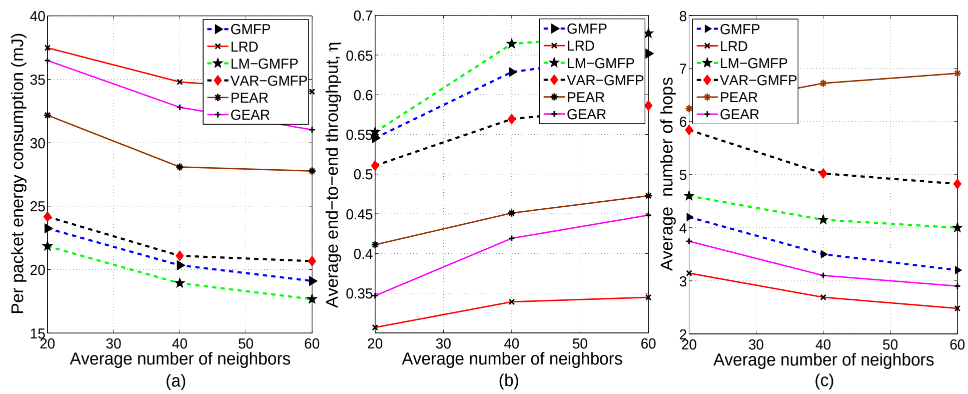

Fig. 5. Network density dependent network performance: (a) energy consumption per successful end-to-end packet delivery; (b) end-to-end throughput (probability of success); (c) average hop count. Nodal communication range $R = 50$ m.

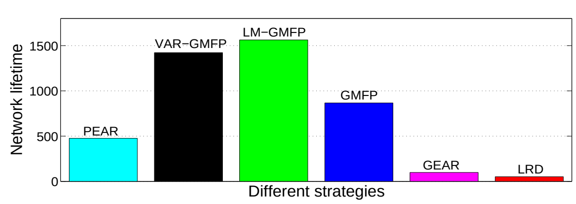

Fig. 6. Network lifetime (number of end-to-end successful packets until the network dies). $R = 40$ m, average number of neighbours $= 20$.

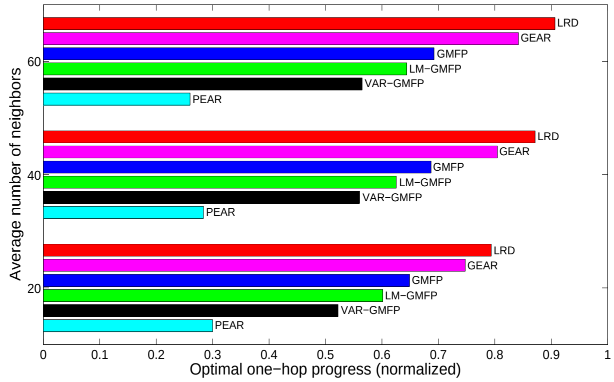

Fig. 7. Average one-hop distance progress in different protocols $R = 40$ m, average number of neighbours 40.

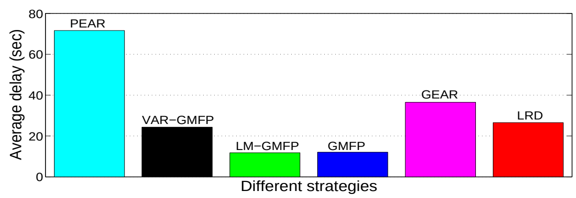

Fig. 8. Average end-to-end delay of different protocols. $R = 40$ m, average number of neighbours 40.

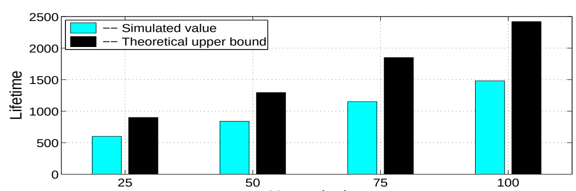

Fig. 9. Theoretical upper bound, as compared to the actual network lifetime in LM-GMFP. $R = 20$ m.